Quantitative Measurement of Manufactured Diamond Shape

Richard Hartley, Alison Noble, James Grande & Jane Liu

G.E. CRD, Schenectady, NY, 12301.

Abstract. We describe a novel application of deformable templates to automatic shape classification of manufactured (man-made) diamonds. We introduce a new shape parameter, τ, to characterize diamond morphology and describe an approach to compute it from images. Our approach has been implemented in an image analysis system which is currently being used on a regular basis to classify diamonds at a manufacturing facility. An experimental evaluation of the system is given.

1 Introduction

Since the invention of manufactured diamonds in 1955 [1] there has been considerable interest in developing methods to grow man-made diamonds which have similar properties to natural diamonds in terms of strength, conductivity and durability but can be manufactured at a reduced cost. Industrial diamonds now out-perform natural diamonds in most applications. They are used in areas such as electronics [2], construction and glass-making [3] and find wide use as abrasives in grinding, sawing and drilling tooling [4, 5]. Increasingly, end-users demand manufactured diamonds which give better performance in products. This translates into a need for diamond manufacturers to improve their understanding of how diamonds perform in applications and how to manufacture a greater proportion of high quality crystals to meet market demand. In particular, the quality of industrial diamonds for use in abrasive applications is dependent on their shape and impurity content [4, 6].

In this paper we present a new and quantitative approach to shape-based quality assessment of sorted diamonds from images. Typical images are shown in Fig. 1a-b. The shape of a diamond with optimal abrasive properties should lie midway between a cube and an octahedron. However, in practice, manufactured diamonds exhibit a wide range of shapes ranging from cubic to octahedral, and irregular and broken shapes also occur. They may also grow in pairs, or become inter-grown by a process called twinning. Although it is possible to exercise some control over the shapes produced by changing the pressure and temperature used in the synthesis process, it is necessary to perform some type of crystal sorting or grading after separation.

Before proceeding further, let us identify three key challenges to machine vision that relate to the development of an automated diamond classification system. These are: (1) how to utilize a measurement model that captures the nature of a 3D diamond crystal; (2) how to develop image analysis techniques that give reliable and repeatable image measurements under a reasonable range

Lecture Notes in Computer Science, Vol. 800
Jan-Olof Eklundh (Ed.)
Computer Vision – ECCV '94

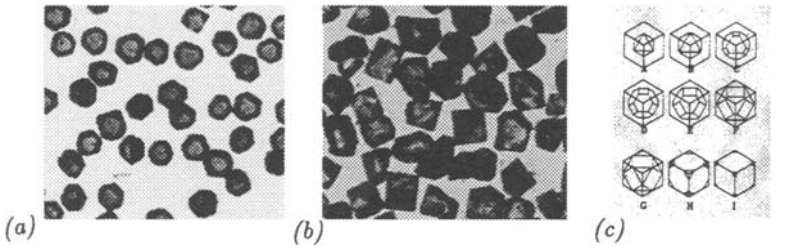

Fig. 1. *Diamond shapes : (a) regular diamonds; (b) irregular ones. (c) Classification scheme based on the change in crystal morphology from an octahedron to a cube.*

of operating conditions; and (3) how to provide fast computation to meet the speed requirements necessary to gather crystal population statistics for production use. In the following sections, we describe an approach developed to meet these three criteria based on deformable templates [7]. Our approach has been translated into a diamond classification system which is being used on a regular basis in a diamond manufacturing facility [8].

2 Crystal Shape Parameters

The form of a regular diamond crystal lies somewhere between a cube (hexahedron) and an octahedron [9, 10]. There is a continuous range of possible shapes. At one extreme is the octahedron which has eight triangular faces and six vertices and at the other is the cube, with six square faces and eight vertices. Intermediate shapes may be regarded as being the intersection of a cube and an octahedron.

Figure 1c indicates a possible *qualitative* diamond classification scheme. Here a diamond is classified into one of a number of discrete shape groups defined by the change in crystal morphology from an octahedron to a cube. Figure 1c shows 9 classes designated by letters A to I which we will refer to as the A–I or octahedron-cube classification scheme. Note that a range of grades would typically be required to characterize a sample of manufactured diamonds using this scheme as the sample may contain a number of different crystal shapes. Further, an ideal scale like this only provides a qualitative and subjective estimate of shape content. Alternatively, as we see next, a more convenient computational model for *quantitative* analysis can be defined by expressing the shape range in terms of a single, continuous parameter which we call the τ parameter.

Definition of the τ Parameter: consider a cube C with sides of length 2 units and vertices at the points $(\pm 1, \pm 1, \pm 1)$. Let a plane pass through $(2\tau - 1, 1, 1)$, $(1, 2\tau - 1, 1)$ and $(1, 1, 2\tau - 1)$. For $\tau \in [0, 1]$ this plane cuts off a neighborhood of the vertex $(1, 1, 1)$ of the cube (in fact, a tetrahedron of height $\frac{2}{\sqrt{3}}(1 - \tau)$). Similar planes cut off the other vertices of the cube. The remaining polyhedron after truncation by these planes is a cubo-octahedron, denoted C_τ. Note that for $\tau = 1$, C_τ is the original cube C, since the truncating planes do not meet the cube except at the vertices. On the other hand, for $\tau = 0$, the polyhedron is an octahedron with one vertex at the center of each of the faces of the original cube. Figure 2a shows the polyhedron C_τ for a value $\tau = 0.7$. For $\tau = 0.5$ the

polyhedron C_τ has a special shape half way between a cube and an octahedron which may be thought of as the transitional stage between essentially cubic and essentially octahedral shapes (Fig. 2b). For $\tau < 0.5$, the truncating planes meet each other, and the truncated regions around each vertex overlap (Fig. 2c).

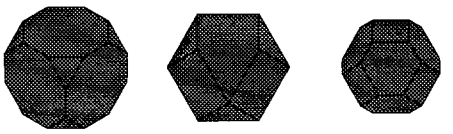

Fig. 2. $\tau = 0.7, 0.5,$ *and* 0.3 *for an ideal crystal viewed perpendicular to the octahedral (111) face.*

Face Types: the faces of C_τ may be classified into two types; those corresponding to faces of the original cube (*cubic*, or (100) faces[1]). and those corresponding to the truncating planes (*octahedral*, or (111) faces).

For τ greater than 0.5, the (111) faces of C_τ do not meet, whereas for $\tau < 0.5$ they do. For $\tau = 0.5$ the (111) faces of C_τ meet at vertices only. The case $\tau = 0.25$ is a useful reference point, since in this case, the (111) faces of C_τ are regular hexagons. The shapes of the various faces of the polyhedron and the approximate correspondence between the octahedron–cube shape designation and the τ parameter are shown in Table 1.

τ value	octahedral faces	cubic faces
$\tau = 0$	triangle	—
$0 < \tau < 0.5$	hexagon	square
$\tau = 0.5$	triangle	square
$0.5 < \tau < 1.0$	triangle	octagon
$\tau = 1.0$	—	square

(a)

Letter	A	B	C
τ	0.0	0.083	0.167
Letter	D	E	F
τ	0.250	0.333	0.417
Letter	G	H	I
τ	0.5	0.7	0.9

(b)

Table 1. *(a) Shapes of faces for cubo-octahedral diamond crystals. (b) Approximate correspondence of the shape designation letters in Fig.1 with τ values.*

3 System and Algorithm for Shape Classification

The system set-up is shown in Fig. 3a. The integrated image analysis system consists of three modules; image acquisition(camera, lighting, framegrabber), analysis (for measuring diamond shape) and classification (for grading the diamond sample as a whole). The software is written in the C++ language and uses the X-toolkit InterViews. Processing time on a Sparc2 workstation is around 1 second per diamond.

[1] using the standard Miller indices notation used in crystallography [4].

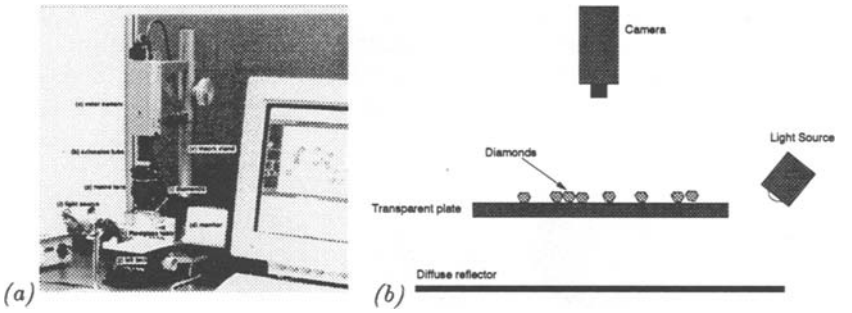

Fig. 3. *(a) Image capturing hardware. (b) Apparatus used for obtaining diamond images.*

3.1 Defining Shape Templates

Assume we view a regular diamond sitting on one of its faces, in a direction perpendicular to this face. If the crystal is back-lit it will have a dark outer band and a brighter interior region corresponding to the upper horizontal face of the diamond (Fig.4). A template is defined in terms of the shape of the inner and outer outlines of these regions. More specifically, a template consists of two polygons which are each dependent on the shape parameter τ. The template representation of a diamond will vary according to whether it is sitting on its octahedral face or its cubic face. It will also vary according to whether τ is less than or greater than 0.5. All possible combinations of polygons are summarized in Table 2. These are used in template matching as part of the algorithm described in the next section.

Top face	τ	Inner Outline	Outer Outline
cubic	< 0.5	square	octagon
cubic	> 0.5	octagon	square
octahedral	< 0.5	hexagon	dodecagon
octahedral	> 0.5	triangle	dodecagon

Table 2. *The four basic diamond templates.*

3.2 Algorithm

Image Capture: the image capture set-up is shown in Fig.3b. Diamonds are lit from below using diffuse light. An image is captured with a video three-channel camera placed above the diamonds and facing downwards. Then the color image is converted into a grey level image using a linear combination of the red, green and blue bands chosen to enable the three regions of the image (background, bright diamond and dark diamond) to be distinguished by thresholding on grey-level values.

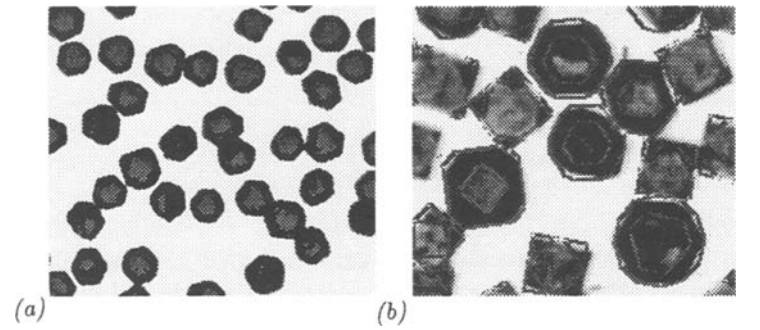

Fig. 4. *(a) Segmented diamond image. (b) Templates fit to imaged diamonds.*

Feature Extraction: the first step in image analysis is separation of the image into three regions, background, dark diamond faces and bright diamond faces (the inner face) using multi-level thresholding. The two thresholds T_1 and T_2 ($T_1 < T_2$) are determined during a pre-analysis calibration stage and only have to be re-calculated when the lighting settings change. After thresholding, the segmentation is cleaned up using morphological operators. Finally, touching diamonds are separated using a morphological algorithm based on the ultimate erosion followed by conditional dilation [11]. Figure 4a shows the result of applying these steps to the image in Fig.1a.

Template Matching: the next task is to determine the value of the parameter τ for which C_τ most closely resembles the actual diamond. This involves fitting the inner and outer outlines of the diamond to a diamond template. A complete placement of the template in the image is determined by the following parameters: the shape parameter τ; the center of the template (x_0, y_0); a rotation r; and a scale factor k. These are varied to find the best fit of the template with the outlines of the actual diamond image. The outer outline is defined by pixels on the boundary between a diamond interior and the background or between touching diamonds. The inner outline is in general less distinct and can not be reliably localized using the threshold T_1. Instead, the intensity gradient is used to determine points on the inner outline which are weighted according to the gradient magnitude. The best fit is found by starting from initial values of the parameters and iterating (using the Levenberg-Marquardt parameter fitting algorithm [12]) to the best fit. The cost function to be minimized is $\sum_p w_p d(x,T)^2$, where $d(x,T)$ is the radial distance between a boundary (fitting) point p and the template T, w_p is a weight representing the strength of the edge pixel p, and the sum runs over all pixels in the inner and outer outlines of the image diamond. The image of the diamond depends on whether it is sitting on its octahedral face or its cubic face. It also varies according to whether τ is less than or greater than 0.5 as indicated in Table 2. It is necessary, therefore, to try several different templates to find the best template fit which has minimal fitting error. Once the best fit has been found, the corresponding value of τ is computed as the diamond classification parameter. Note that the templates are fitted to give the best approximation to a regular shape and not fitted to the diamond outlines

exactly. Hence, the fit is very good for regular diamonds but can be poor for irregular diamonds. An example of template fitting is shown in Fig.4b.

4 Experiments

In this section we describe results from a series of experiments carried out to test the performance of the diamond classification software. Diamond samples were kindly provided by GE Superabrasives, Worthington, OH.

1. Diamonds with Different Cubo-Octahedral Shapes: hand-picked crystal samples with shapes conforming to only one of the letters A–I in Fig. 1c were used to verify that the τ-based algorithm obtained substantially the same grading as a human observer. Since it is extremely tedious and time-consuming to hand-pick diamonds, the sample sets were quite small. Histograms of τ estimates for five samples (corresponding approximately to the shapes designated D,E,F,H,I in Fig.1) are shown in Fig.5. The mean of the distribution of τ in the different categories agrees well with the approximate theoretical values given in Table 1b.

2. Consistency Test: the algorithm was run five times on samples of about sixty diamonds from each of two machine-separated diamond samples. Sample set *Shape1* contained more regular crystals than *Shape2*. The shape factor, τ, was computed and plotted as a histogram (to show the statistical variation in the sample). Between runs, the sample was shaken up so that the diamonds would be in different orientations for each run. The histogram plots in Fig. 6 show the results of five different runs on sample set *Shape1* and *Shape2*. Observe that the results are quite consistent across the different runs showing the repeatability of measurement w.r.t. crystal orientation. Note also that the spread is greater for *Shape2* than for *Shape1* due to the presence of more irregular crystals in the former sample set.

	Actual	
	low τ %	high τ %
cube	50	50
shape3	35	65

	Actual		Estimate	
	low τ %	high τ %	cube %	shape3 %
shape3 (40%)	10.17	89.83	44.2	55.8
shape3 (60%)	81.61	18.39	65.2	34.8

Table 3. *Mixture sample analysis.*

3. Mixture Samples: three further samples were prepared to test how well the system can determine the proportions of different diamond shapes present in a given sample. These were a sample *Cube* of 60 diamonds containing about 90% cubic-shaped crystals; a sample *cube40_shape3* of 60 diamonds containing (exactly) 40% of diamonds from the sample *Cube* and 60% of diamonds from a machine-separated sample *Shape3*; and a sample *cube60_shape3* of 60 diamonds containing (exactly) 60% of diamonds from the sample *Cube* and 40% of diamonds from a machine-separated sample *Shape3*. Histogram plots of estimated

τ values are plotted in Fig.7. Note that the distributions of the mixed samples clearly show the difference between the two types of diamonds.

The distributions were analyzed to determine the proportions of the two samples in the mixtures (Table 3). Briefly, the four histograms were divided into "low-τ" ($\tau < 0.4$) and "high-τ" ($\tau \geq 0.4$). Note that the percentage of low-τ diamonds (10.17%) agrees closely with the supposed proportion (10%) of non-cubic diamonds in the *Cube* sample. By solving a simple linear equation the mixture proportions may be determined. The results are also shown on the right in Table 3. In particular, it is estimated that the *cube40_shape3* sample contains 44.2% of cubic diamonds, and the *cube60_shape3* sample contains 65.2% of cubic diamonds. These are relatively close to the exact values. A repetition of this experiment using different samples gave better estimates of 38.9% cubic diamonds for *cube40_shape3* and 62.25% cubic diamonds for *cube60_shape3*.

Conclusion: The algorithm performed very well on the assigned tasks and is quite robust. Tests show that the algorithm is capable of effectively distinguishing between diamonds in the octahedron-cube (A–I) classification scheme and can characterize the difference between machine-separated samples.

Acknowledgements: We thank Bill Banholzer, Steve Hayden and Bill Jackson for providing the problem for us to work on and Eric Lifshin for his continued support throughout the project.

References

1. H.P. Bovenberk, F.P. Bundy, H.T. Hall, H.M. Strong, and R.H. Wentorf. Preparation of Diamond. *Nature*, 184:1094–1098, October 1959.
2. J. Spehar. Diamonds, electronics' best friend. *IEEE Potentials*, 10:9–12, 1991.
3. H. Wapler and H.O. Juchem. Diamond abrasives for machining glass. *Industrial Diamond Review*, 47:159–162, 1987.
4. J. Wilks and E. Wilks. *Properties and Applications of Diamond.* Butterworth Heinemann Ltd., Oxford,England, 1992.
5. D.N. Wright and H. Wapler. Investigations and prediction of diamond wear when sawing. *Industrial Diamond Review*, 5:213–216, 1986.
6. J.E. Field. *The properties of natural and synthetic diamond.* Academic Press, London,England, 1992.
7. A.L. Yuille, D.S. Cohen, and P.W. Hallinan. Feature Extraction from Faces using Deformable Templates. In *Proceedings of the IEEE Conference on Computer Vision and Pattern Recognition*, pages 104–109, San Diego, CA., June 1989.
8. W.E. Jackson and S.C. Hayden. Quantifiable Diamond Characterization Techniques: Shape and Compressive Fracture Strength. In *Diamond and CBN Ultrahard Materials Symposium '93*, Windsor, Ontario, Canada, September 1993.
9. S. Yamaoka, H. Komatsu, H. Kanda, and N. Setaka. Growth of Diamond with Rhombic Dodecahedral Faces. *Journal of Crystal Growth*, 37:349–352, 1977.
10. M. Moore. Diamond morphology. *Industrial Diamond Review*, 45:67–71, 1985.
11. J. Serra. *Image Analysis and Mathematical Morphology.* Academic Press, London, England, 1982.
12. W.H. Press, B.P. Flannery, S.A. Teukolsky, and W.T. Vetterling. *Numerical Recipes in C: The Art of Scientific Computing.* Cambridge University Press, 1988.

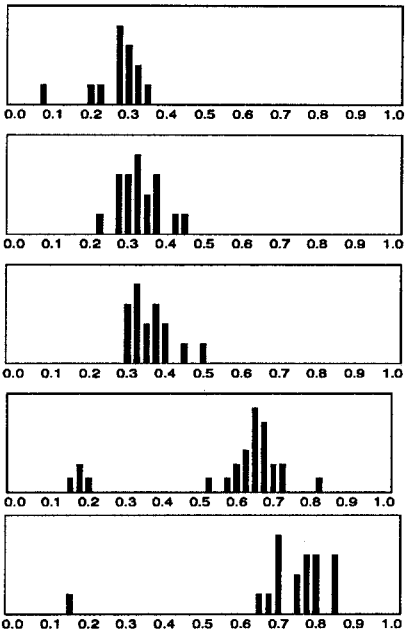

Fig. 5. *Histogram plots of the shape parameter τ for hand-picked samples of (from the top) shape designations D, E, F, H and I in Fig. 1.*

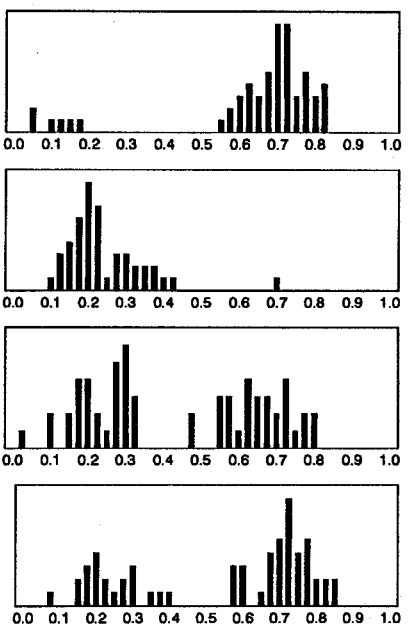

Fig. 7. *Histogram plot of the shape parameter τ for mixture samples. From the top: cube; shape2; 40% cube/60% shape2; 60% cube/40% shape2.*

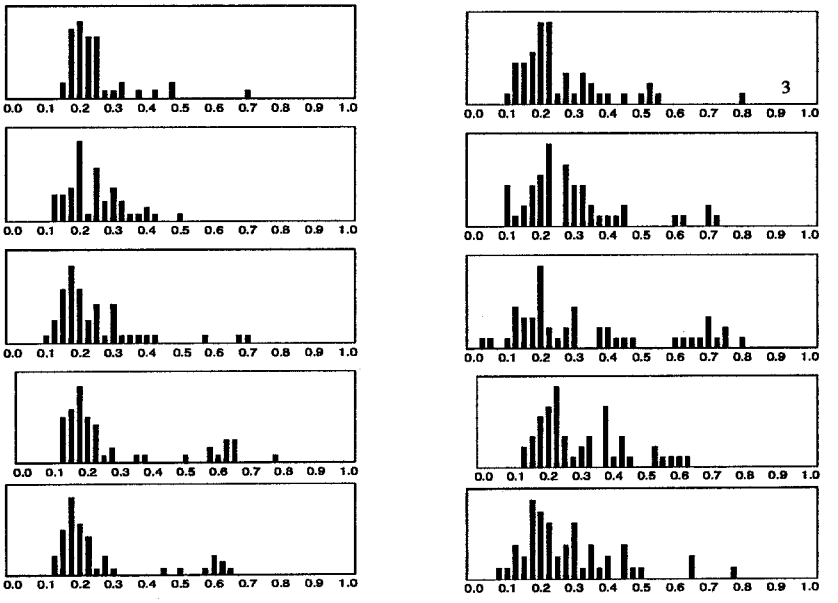

Fig. 6. *Histogram plot of the shape parameter τ for Shape1 (left) and Shape2 (right) diamonds in 5 runs.*